IEEE Access
Multidisciplinary ⋮ Rapid Review ⋮ Open Access Journal

Received December 11, 2019, accepted December 26, 2019, date of publication January 7, 2020, date of current version January 15, 2020.

Digital Object Identifier 10.1109/ACCESS.2020.2964561

The Flexibility of the Generalized Gamma Distribution in Modeling the Fading Based on Kullback-Leibler and Kolmogorov-Smirnov Criteria

ZABIHOLLAH HASANSHAHI[1], PAEIZ AZMI[2], (Senior Member, IEEE), MOHAMMAD HOSSEIN GHOLIZADEH[3], AND MOHAMMAD KHAJEZADEH[4]

[1]Telecommunication Research Institute of Iran, Tehran 1653734165, Iran
[2]Department of Electrical and Computer Engineering, Tarbiat Modares University, Tehran 14115, Iran
[3]Department of Electrical Engineering, Vali-e-Asr University of Rafsanjan, Rafsanjan 7718897111, Iran
[4]Department of Electrical Engineering, Amirkabir University of Technology, Tehran 15875-4413, Iran

Corresponding author: Paeiz Azmi (pazmi@modares.ac.ir)

ABSTRACT The precision of Rayleigh distribution, as the simplest fading model in Non-Line-of-Sight (NLOS) channels, is low in high-resolution radars and long-distance communication receivers. Many currently-available statistical models with a higher precision, including Nakagami-m, Weibull and generalized hybrid Gamma models, are used to describe the radar clutter and the reflected signals in communication receivers. Although the mentioned models in NLOS channels have more accurate matching with the actual fading, a variety of models and the lack of a comprehensive model in different fading channels make it difficult to select an appropriate model. In this paper, the generalized Gamma model is analyzed and evaluated to demonstrate that it adapts to other fading models. Moreover, it also matches with long-term fading, as well as combined long and short-term fading models. Using a practical sample, it is stated that the generalized Gamma model is also adaptable to the channels to which none of the other available closed-form models are suitable. The simulations and the real data results, approved by Kullback-Leibler and Kolmogorov-Smirnov criteria, prove the claim.

INDEX TERMS NLOS channel, fading model, generalized Gamma distribution, Kolmogorov-Smirnov criterion.

I. INTRODUCTION

The propagation of electromagnetic waves in wireless channels develops complicated phenomena such as shadowing and multipath. The impossibility of presenting an accurate mathematical description for these phenomena, due to the stochastic nature, makes the analysis of the communication and radar systems complicated [1]. Nevertheless, the modelling of the fading and shadowing is essential to analyze wireless communication problems including analyzing the cellular systems, the performance of multiple-input and multiple-output (MIMO) networks, and the performance of tracking and navigation systems in Non-Line-of-Sight (NLOS) channels in which the distance measurements are contaminated with NLOS errors [2]–[4]. Some considerable efforts are made to statistically model the features of the above effects. Consequently, a wide range of relatively-simple and accurate statistical models is determined and extracted for fading channels in a specific propagation medium under a special communication scenarios [1]. Small-scale multipath fading is often modelled using Rayleigh, Rician and Nakagami-m models, and large-scale fading (shadowing) is modelled based on a log-normal distribution [2], [3].

The amplitude distribution of the fully-developed reflected signals follows a Rayleigh distribution. Nevertheless, non-Rayleigh distribution is observed in many cases, including when the number of scatters is small in a cell resolution and the scatters are organized based on a certain type of repeatability, or when scatters constitute the dominant components in a cell. There is a group of simple and hybrid

The associate editor coordinating the review of this manuscript and approving it for publication was Jiayi Zhang.

distributions used to statistically model the non-Rayleigh distribution of amplitude, including Nakagami, Rician, lognormal, K and generalized K [5], [6]. Using the lognormal distribution and the Rayleigh distribution to model the shadowing, and the small-scale fading, respectively, results in a hybrid Rayleigh-lognormal distribution. Given that the form of the related function is not closed, the Gamma distribution is used instead of the lognormal, which develops the K distribution.

Using the Gamma distribution to model the shadowing, and the Nakagami distribution for modeling the small-scale random variables related to the envelope of the received signals results in a closed-form of the hybrid fading probability density function (PDF), namely the Gamma-Gamma distribution (GK) [3]. The generalized Rayleigh (GR) distribution is employed to model the long-terms and small-terms of the signal variables. GR distribution has a simple mathematical expression, and includes the Rayleigh distribution as a special case. It also can be used instead of Rayleigh-Lognormal (RL) and K distributions, and therefore, obviates the need for using other distributions in wireless channels to model fading [7]. The $\kappa-\mu$ shadowed distribution also has a strong flexibility to model different propagation conditions in wireless environments. This model unifies all the classic fading models, i. e., the one-sided Gaussian, Rayleigh, Nakagami-m, Nakagami-q, Rician, their generalized counterparts, the $\kappa-\mu$, $\eta-\mu$ and Rician shadowed fading models [8], [9]. The generalized Gamma (GG) distribution includes Gamma and exponential distributions, and is presented as the Weibull distribution in a special case, and as the lognormal distribution in a limited case [10].

This paper, based on the tests performed on real data related to faded signals in the second generation (2G) network [11], shows that the GG distribution has a higher flexibility compared to simple and closed-form distributions, like GK and GR, in adapting to RL and K distributions. The simple and closed-form of the GR distribution facilitates the analysis and the design of communication systems; nevertheless, comparing the results associated with the adaptation of the GR with RL and K distributions [7] with those associated with the adaptation of the GG distribution with these models suggests that the GG distribution is more flexible in adapting to the cited hybrid models. In addition, GG model covers other fading models, including Gamma, Weibull and exponential, and offers an appropriate closed-form for analyses and evaluations. The mentioned adaptation is performed using goodness of fit (GOF), such as the Kolmogorov-Smirnov (K-S) criterion [12]. Some of the results are, however, investigated using other criteria, including Kullback-Leibler (KL) and Anderson-Darling (A-D) [13], [14]. A practical experiment also demonstrates that the GG model is statistically more adaptable to the received data in NLOS channels compared to the hybrid models discussed.

The rest of the paper is organized as follows: In section II, various hybrid distributions of fading and shadowing are introduced and investigated. Section III demonstrates a higher degree of compatibility of the GG distribution compared to that of the simple distributions such as GR, and relatively complex distributions such as $\kappa-\mu$ shadowed distribution in similarity to the K and RL based on KL criteria [8], [9], [15]–[19]. Section IV investigates the signals received from the directional antenna of cellular network transmitters associated with the main, side and back lobes on the LOS/NLOS and NLOS channels under a multipath condition. Moreover, the deviation from the Rayleigh distribution is explored based on the Jakeman criterion [20], [21], and the flexibility of each model with the practical data is shown based on the K-S criterion. The paper is concluded in Section V.

II. NON-RAYLEIGH MODELS FOR STOCHASTIC CHANNELS

Interfering waves received in a communication channel subject to the multipath phenomenon are represented as [20]:

$$E = X + jY = Ae^{j\varphi} = \sum_{i=1}^{N} a_i e^{j\varphi_i}, \tag{1}$$

in which N represents the number of the reflected signals in a cell. a_i and ϕ_i are the reflected amplitude and phase from the ith path, respectively. X and Y are the real and imaginary parts of the reflected signal, respectively [20]. When the number of independent interfering signals, i.e. reflected signals from independent obstacles, is small, the central limit theorem does not hold and the distribution of the signal envelope deviates from Rayleigh. The N value should therefore exceed a special threshold to realize the Rayleigh distribution for limited N [20]:

$$\begin{aligned} N &>> \frac{R^4}{4}|\beta-2| \\ \beta &= m_4/{m_2}^2 = \left\langle E_j^4 \right\rangle / \left\langle E_j^2 \right\rangle^2, \end{aligned} \tag{2}$$

in which R represents the Rayleigh constant, $\langle . \rangle$ denotes the expectation value, E_j is the amplitude of the jth reflected signal, and m_2 and m_4 are the second-order and fourth-order moments of the probability distribution E_j, respectively. As $N \rightarrow \infty$, the distribution approaches the pure Rayleigh [20].

The conditions for realizing the Rayleigh distribution in many other instances, when the number of reflected interfering waves is not constant and changes instantly, is as [20]:

$$\frac{\langle N^2 \rangle}{\langle N \rangle^2} \rightarrow 1. \tag{3}$$

In this case, N is Poisson-distributed, and we have [20]:

$$\frac{\langle N^2 \rangle}{\langle N \rangle^2} = \frac{1}{\langle N \rangle} + 1. \tag{4}$$

When $\langle N \rangle >> 1$, the equation (4) approaches 1, and therefore, the equation (3) will hold. When deviating from Rayleigh, a mean effective number of scatterers, i. e., $N_{eff}(r)$,

is defined that affects the statistical behavior of the received signal, and we have [21], [22]:

$$\frac{\langle \sigma^2(r) \rangle}{\langle \sigma\ (r) \rangle^2} = 2\left(1 - \frac{1}{N}\right) + \frac{1}{N_{eff}(r)}, \tag{5}$$

in which N represents the number of reflected signals, and $\sigma^i(r)$ is the ith moment of the reflected signal. According to equation (5), deviation from Rayleigh is relatively low for $N_{eff} > 10$, and significant for $N_{eff} \sim 1$ [22]. Thus, N_{eff}/N can be employed as a criterion based on the moments. The Kullback-Leibler divergence and Kolmogorov-Smirnov criteria are also used to determine the deviation from Rayleigh.

In the following, some non-Rayleigh models are discussed, including K, F, GK, GR, $\eta - \mu$, $\kappa - \mu$, $\kappa - \mu$ shadowed and GG.

A. K DISTRIBUTION

Given the complexity of the Rayleigh-Lognormal equation, the Gamma distribution is used instead of the lognormal to obtain a closed-form equation, resulting in the K distribution as [22, eq. 22]:

$$f_\kappa(x) = \frac{2d}{\Gamma(c)}\left(\frac{dx}{2}\right)^c K_{c-1}(dx). \tag{6}$$

in which $\Gamma(.)$ represents the Gamma function and K_ν is the modified second-order Bessel function of degree ν. The parameters c and d also respectively denote the shape and scale parameters of the K function [22]. It can be shown that K distribution approaches to the Rayleigh distribution for $c > 20$ [23].

B. F DISTRIBUTION

The probability density function of the signal envelope, called F distribution, is obtained by averaging the infinite integral of the conditional PDF of the Nakagami-m distribution with respect to the random variation of the *rms* signal power, and finally, is demonstrated as [24]:

$$f_X(x) = \frac{2m^m (m_s\Omega)^{m_s} x^{2m-1}}{B(m, m_s)(mx^2 + m_s\Omega)^{m+m_s}}, \tag{7}$$

in which m is the fading severity parameter, m_s is the shape parameter of the related Nakagami-m distribution, $\Omega = E[x^2]$ is the the mean power, and $B(\cdot, \cdot)$ is the beta function [24].

C. THE GK DISTRIBUTION

The Gamma-Gamma or Generalized-K model is derived from the F distribution by converting the signal mean power model to the Gamma distribution. The generalized-K model is expressed as [3]:

$$f_X(x) = \frac{4m^{(\beta+1)/2} x^\beta}{\Gamma(m)\Gamma(k)\Omega^{(\beta+1)/2}} K_\alpha\left[2\left(\frac{m}{\Omega}\right)^{1/2} x\right], \tag{8}$$

in which $\alpha = k - m$ and $\beta = k + m - 1$, m and k represent the shape parameters, and $\Omega = E\left\langle X^2 \right\rangle / k$ is the average power. As stated earlier, $\Gamma(\cdot)$ represents the Gamma function, and K_ν is the modified Bessel function of the second-order and degree ν [3].

D. THE GR DISTRIBUTION

The GR distribution is used for both short and long-term fading in wireless channels. It has simple mathematical closed-form, and simplifies the calculation of parameters such as bit error rate (*BER*). The GR distribution is given in [7]:

$$f\ (x; \alpha, a) = \frac{r\ (1+a)}{\alpha} \frac{\exp\left\{x^2/(2\alpha)\right\}}{\left[(1+a)\exp\left\{x^2/(2\alpha)\right\} - a\right]^2}, \tag{9}$$

in which $\alpha > 0$ and $a > 0$ are the shape and scale parameters, respectively, and $x \geq 0$. The function is converted to the Rayleigh function when a approaches zero [7].

E. THE η — μ DISTRIBUTION [15]

Let γ be a random variable that statistically is $\eta - \mu$ distributed with mean $\bar{\gamma}=E[\gamma]$ and non-negative real shape parameters η and μ, i. e., $\gamma \sim S_{\eta\mu}(\bar{\gamma}; \eta, \mu)$, and the related PDF is given by [15]:

$$f_\gamma(\gamma) = \frac{\sqrt{\pi}(1+\eta)^{\mu+\frac{1}{2}}\mu^{\mu+\frac{1}{2}}}{\Gamma(\mu)\bar{\gamma}\sqrt{\eta}(1-\eta)^{\mu-\frac{1}{2}}}\left(\frac{\gamma}{\bar{\gamma}}\right)^{\mu-\frac{1}{2}} \times e^{-\frac{\mu(1+\eta)^2\gamma}{2\eta\bar{\gamma}}} I_{\mu-\frac{1}{2}}\left(\frac{\mu\left(1-\eta^2\right)}{2\eta}\frac{\gamma}{\bar{\gamma}}\right), \tag{10}$$

where $I_\nu(\cdot)$ is the ν-th order modified Bessel function of the first kind, which can be defined in terms of the Bessel hypergeometric function ${}_0F_1(.)$ [16, eq. 9.6.47].

F. THE κ — μ DISTRIBUTION [15]

Let γ be a random variable that statistically is $\kappa - \mu$ distributed with mean $\bar{\gamma}=E[\gamma]$ and non-negative real shape parameters κ and μ, i. e., $\gamma \sim S_{\kappa\mu}(\bar{\gamma}; \kappa, \mu)$, and the related PDF is as [15]:

$$f_\gamma(\gamma) = \frac{\mu(1+\kappa)^{\frac{\mu+1}{2}}}{\bar{\gamma}\kappa^{\frac{\mu-1}{2}}e^{\mu\kappa}}\left(\frac{\gamma}{\bar{\gamma}}\right)^{\frac{\mu-1}{2}} \times e^{-\frac{\mu(1+\kappa)\gamma}{\bar{\gamma}}} I_{\mu-1}\left(2\mu\sqrt{\frac{\kappa\ (1+\kappa)\ \gamma}{\bar{\gamma}}}\right). \tag{11}$$

G. THE κ — μ SHADOWED DISTRIBUTION [8], [9]

Let γ be a random variable that statistically is $\kappa - \mu$ shadowed distributed with mean $\bar{\gamma}=E[\gamma]$ and non-negative real shape parameters κ, μ and m, i. e., $\gamma \sim S_{\kappa\mu m}(\bar{\gamma}; \kappa, \mu, m)$, and the related PDF is given by [9]:

$$f_\gamma(\gamma) = \frac{\mu^\mu m^m (1+\kappa)^\mu}{\Gamma(\mu)\bar{\gamma}(\mu\kappa+m)^m}\left(\frac{\gamma}{\bar{\gamma}}\right)^{\mu-1} \times e^{-\frac{\mu(1+\kappa)\gamma}{\bar{\gamma}}} {}_1F_1\left(m; \mu; \frac{\mu^2\kappa\ (1+\kappa)}{\mu\kappa+m}\frac{\gamma}{\bar{\gamma}}\right), \tag{12}$$

where ${}_1F_1(.)$ is the confluent hypergeometric function of scalar argument [16, eq. 13.1.2], which is a particular case of the generalized hypergeometric function [8].

H. THE GG DISTRIBUTION

The distribution of the Gamma family is popular in analyzing the skewed data. The GG distribution was introduced by Stacy in 1962, and includes exponential, Weibull, Gamma and Rayleigh models. The GG distribution is employed to model data with dissimilar hazard rates. The probability density function of GG distribution is as [25]:

$$f_X(x) = \frac{\alpha_2}{\Gamma(\alpha_1)\beta}\left(\frac{x}{\beta}\right)^{\alpha_1\alpha_2-1}\exp\left[-\left(\frac{x}{\beta}\right)^{\alpha_2}\right], \quad for\ x>0;\ \alpha_1,\alpha_2,\beta>0 \tag{13}$$

in which α_1 and α_2 represent the shape parameters and β is the scale parameter [25], [26]. Another formulation for the GG distribution is as [10]:

$$f_X(x) = \frac{2\nu x^{(2\nu m-1)}}{\Gamma(m)(\Omega/m)}\exp\left(-\frac{mx^{2\nu}}{\Omega}\right) \quad x\geq 0 \tag{14}$$

in which $\nu = \frac{\alpha_2}{2}$, $m = \alpha_1$ and $\Omega = \alpha_1\left(\beta^{\frac{1}{\alpha_2}}\right)$.

III. THE FLEXIBILITY OF THE GG DISTRIBUTION IN SIMILARITY TO THE K AND RL

Although the RL distribution is demonstrated to be useful for modeling the shadowing in wireless channels, the K distribution is introduced as an alternative to the RL distribution because of the related closed-form and the similarity to the RL distribution [27]. The GR model is also proposed given the better similarity to the RL [7]. Based on the KL criterion, this section shows that the GG distribution is better adapted to the RL and K distributions compared to the GR distribution.

A. THE CRITERION OF KULLBACK-LEIBLER DIVERGENCE

For absolutely-continuous probability density functions of f and g over the domain of $\mathbb{R}^n$ with the following conditions:

$$f(x) = 0 \rightarrow g(x) = 0, \tag{15}$$

the relative entropy or the criterion of Kullback-Leibler divergence (KLD) is as [13]:

$$D_{KL}(f||g) = \int_0^\infty f(x)\log\left\{\frac{f(x)}{g(x)}\right\}dx. \tag{16}$$

The following assumptions are considered for simplifying:

$$D_{KL}(f||g) = \begin{cases} 0 & \frac{f(x)}{g(x)} = \frac{0}{0} = 1 \\ \infty & f(x)\ is\ not\ absolutely\ continuous. \end{cases} \tag{17}$$

Given the asymmetry of the KL criterion, the Jensen-Shannon divergence (*JSD*) criterion is employed to have a more effective comparison [28]:

$$D_{JSD}(f||g) = \frac{1}{2}\left(D_{KL}(f||m) + D_{KL}(g||m)\right), \tag{18}$$

in which $m = \frac{1}{2}(f+g)$.

On the other hand, the integral square error (*ISE*) is as [29]:

$$D_{ISE}(f||g) = \int_0^\infty (f(x)-g(x))^2\,dx. \tag{19}$$

Thus, both *JSD* and *ISE* criteria are used to compare the results.

B. COMPARING THE RESULTS OF GG, GR, $\eta-\mu$, $\kappa-\mu$ AND $\kappa-\mu$ SHADOWED IN SIMILARITY TO THE RL

To compare $RL(\mu,\sigma)$, $K(c,d)$, $GR(\alpha,a)$, $S_{\eta\mu}(\bar{\gamma}_3;\eta,\mu_3)$, $S_{\kappa\mu}(\bar{\gamma}_2;\kappa_2,\mu_2)$ and $S_{\kappa\mu m}(\bar{\gamma}_1;\kappa_1,\mu_1,m)$ with the function $GG(\upsilon,m,\Omega)$, the values -0.2, 0.3 and 0.9 were first used as the shape parameter d, and the value 2 for the parameter c according to what discussed in [7], [27], [30].

Table 1 presents the values of the parameters of the discussed distributions estimated using the moment method. Table 2 presents the degree of similarity among the functions by using the ISE and JSD values. According to [7], the *GR* distribution is closest to the *RL* distribution, and the results in Tables 1 and 2 approximately confirm it for the interval of $-0.2 \leq d \leq 0.9$.

TABLE 1. Estimating the distribution parameters of *K*, *GR*, $\eta-\mu$, $\kappa-\mu$, $\kappa-\mu$ shadowed and *GG* for $c=2$ and $-0.2\leq d\leq 0.9$.

d	-0.20	0.30	0.90
μ	1.260	1.966	2.462
σ	1.102	0.873	0.724
a	13.788	5.142	2.716
α	32.757	29.463	31.450
ν	1.491	1.927	2.047
m	0.485	0.492	0.521
Ω	2.624	3.584	4.923
$\bar{\gamma}_1$	2.733	3.679	4.579
κ_1	0.250	0.055	-7.42e-06
μ_1	1.401	1.877	2.230
m	1.281	0.478	1.504
$\bar{\gamma}_2$	2.733	3.679	4.578
κ_2	0.443	1.945	2.435
μ_2	1.269	1.050	1.105
$\bar{\gamma}_3$	2.733	3.679	4.578
η	0.969	1.000	1.002
μ_3	0.700	0.931	1.111

TABLE 2. The numerical values of integral square error (*ISE*) and Jensen-Shannon divergence (*JSD*) for the *K*, *GR*, $\eta-\mu$, $\kappa-\mu$, $\kappa-\mu$ shadowed and *GG* distribution in the interval $-0.2\leq d\leq 0.9$.

d	-0.20	0.30	0.90
JSD			
K	0.0054	0.0014	4.464e-04
GR	5.446e-04	5.446e-04	4.834e-04
$\eta-\mu$	0.0404	0.0264	0.0191
$\kappa-\mu$	0.0087	0.0073	0.0037
$\kappa-\mu\ sh.$	0.0062	0.0014	0.0003
GG	0.0057	0.0014	4.493e-04
ISE			
K	0.0060	0.0011	2.690e-04
GR	4.520e-04	1.580e-04	1.700e-04
$\eta-\mu$	0.0747	0.0252	0.0123
$\kappa-\mu$	0.0097	0.0049	0.0016
$\kappa-\mu\ sh.$	0.0068	0.0011	0.0001
GG	0.0062	0.0011	2.700e-04

However, the comparison is now performed for the interval $1.2\leq d\leq 2.2$. Table 3 presents the parameters of the model

TABLE 3. Estimating the distribution parameters of *K*, *GR*, $\eta-\mu$, $\kappa-\mu$, $\kappa-\mu$ shadowed and *GG* for $c = 2$ and $1.2 \leq d \leq 2.2$.

d	1.2	1.5	2.0
μ	2.643	2.798	3.013
σ	0.674	0.632	0.578
a	2.171	1.802	1.397
α	33.111	34.975	38.350
ν	0.538	0.555	0.583
m	2.034	2.001	1.927
Ω	5.704	6.565	8.179
$\bar{\gamma}_1$	4.970	5.333	5.890
κ_1	1.086	1.039	0.766
μ_1	2.171	2.192	2.452
m	3.035	3.794	3.796
$\bar{\gamma}_2$	4.970	5.333	5.890
κ_2	2.521	2.136	1.120
μ_2	1.146	1.319	1.880
$\bar{\gamma}_3$	4.970	5.333	5.890
η	0.999	0.999	1.000
μ_3	1.176	1.231	1.304

TABLE 4. The numerical values of *ISE* and *JSD* for the *K*, *GR*, $\eta-\mu$, $\kappa-\mu$, $\kappa-\mu$ shadowed and *GG* distribution in the interval $1.2 \leq d \leq 2.2$.

d	1.2	1.5	2.0
JSD			
K	3.03e-04	2.08e-04	1.22e-04
GR	5.83e-04	5.68e-04	5.26e-04
$\eta-\mu$	0.0171	0.0156	0.0138
$\kappa-\mu$	0.0026	0.0016	3.08e-04
$\kappa-\mu\ sh.$	3.05e-04	2.20e-04	2.00e-04
GG	3.03e-04	2.28e-04	1.70e-04
ISE			
K	1.56e-04	9.66e-05	4.81e-05
GR	1.65e-04	1.53e-04	1.31e-04
$\eta-\mu$	0.0097	0.0079	0.0061
$\kappa-\mu$	0.0010	5.70e-04	1.14e-04
$\kappa-\mu\ sh.$	1.66e-04	1.09e-04	5.52e-05
GG	1.64e-04	1.10e-04	6.81e-05

estimated using the moment method. The *ISE* and *JSD* values in Table 4 are used to compare the degree of similarity of the functions. According to the Tables 3 and 4, in this interval the *GG* distribution is closer to the *RL* distribution than the *GR* distribution.

On the other hand, Fig. 1 also shows that the *GG* distribution is more similar to the *K* distribution than the *GR* distribution over the interval of $1.2 \leq d \leq 2.2$. Based on [27], due to the relationship between the K and RL distributions, the *GG* distribution is also more similar to the *RL* distribution than the *GR* distribution over the mentioned interval.

Note that, a reliable result, close to K and RL, is also achieved based on some models such as $\kappa-\mu$ shadowed distribution. However, the great number of the related parameters results in a great deal of computational complexity, although some efforts have been made to simplify them in specific applications [17]–[19].

IV. FLEXIBILITY OF THE GG DISTRIBUTION IN MODELLING THE FADING

A. KOLMOGOROV-SMIRNOV (K-S) COMPATIBILITY CRITERION

For n samples of a random variable X, i. e., $X_1, \ldots, X_n$, with $X_1 < X_2 < \ldots < X_n$, the empirical distribution function (EDF) is defined as [31]:

$$F_n(x) = \frac{number\ of\ observations \leq x}{n}. \tag{20}$$

EDF is a statistic that measures the difference between $F_n(x)$ and the distribution function $F(x)$. The Kolmogorov-Smirnov convergence is shown as [12]:

$$D = \sup_x |F_n(x) - F(x)|. \tag{21}$$

In the above criterion, the term alpha level is used to refer to a pre-chosen probability, and the term P-value is employed to indicate a probability that you calculate after a given study [12].

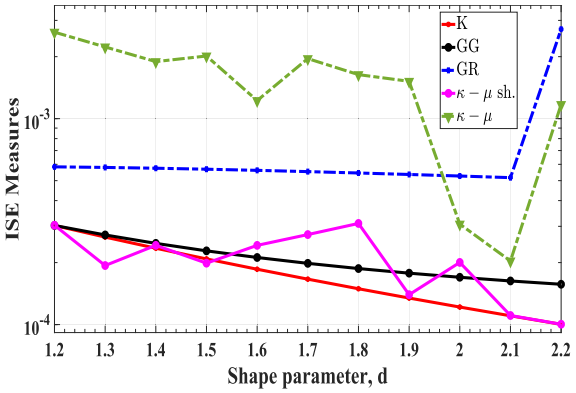

FIGURE 1. The compatibility of the *K*, *GR*, $\kappa-\mu$, $\kappa-\mu$ shadowed and *GG* function based on *ISE* for $1.2 \leq d \leq 2.2$.

B. SAMPLE OF PRACTICAL DATA

Due to the robustness of signals to multi-path propagation and fading in the fourth generation (4G) and fifth generation (5G) networks in comparison with 2G network, two signals related to the two base transceiver stations (BTS) with absolute radio frequency channel number (ARFCN) 50 in LOS / NLOS mode and ARFCN 48 in NLOS mode are employed in 2G network to obtain more realistic results from the fading effect and more precise comparison among different fading models [11]. In cellular communication systems, due to urban barriers in the signal propagation environment, the channel response is stochastic and unknown at different time intervals. Thus, every channel estimation algorithm, including blind and non-blind, should estimate the channel response reliably using a few number of the received samples. The blind methods are not used in practical global system for mobile communications (GSM) [32]. More information about GSM networks are accessible in [33]. These kind of systems, that are time-division multiple access (TDMA) - based, send and receive the data bits as burst. As depicted in Fig. 2, in the

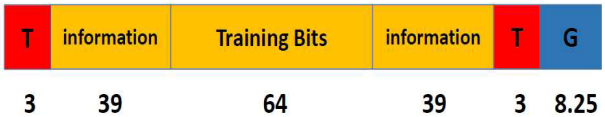

FIGURE 2. The SCH burst framing [33].

broadcast control channel (BCCH) in GSM network, there are synchronization channel (SCH) bursts including predefined bits to synchronize the receiver and transmitter. The training bits in a (one) SCH burst are as [33]:

$$\begin{aligned} \textit{Training bits} = [&1,0,1,1,1,0,0,1,0,1,1,0,0,0,1,0,\\ &0,0,0,0,0,1,0,0,0,0,0,0,1,1,1,1,\\ &0,0,1,0,1,1,0,1,0,1,0,0,0,1,0,1,\\ &0,1,1,1,0,1,1,0,0,0,0,1,1,0,1,1]. \end{aligned}$$

Suppose that the above training bits are equivalent to the signal $S_t(n)$. After Gaussian Minimum Shift Keying (GMSK) modulation, the signal is transmitted. At receiver, after decoding the received GSM signal and tracking the SCH bits, the received signal $S_r(n)$ is obtained that is equivalent to the training bits. For a frequency band in which the transmitted signal is nonzero, the channel is estimated as:

$$\begin{aligned} s_r(n) &= h(n) * s_t(n) \\ h(n) &= F^{-1}\left\{S_r(e^{jw})/S_t(e^{jw})\right\}, \end{aligned} \tag{22}$$

in which "$*$" denotes the convolution operator, $h(n)$ is the channel impulse response, F^{-1} is the Fourier inverse function, $S_r(e^{jw})$ is the Fourier transform of $S_r(n)$ and $S_t(e^{jw})$ is the Fourier transform of $S_t(n)$. Since the signal is sampled with the rate of $\frac{1}{T_s} = 270\ Kbit/s$, each channel tap is equivalent to $T_s = 3.7\mu s$ in the channel estimation. Fig. 3 illustrates the location of the test point and the base transceiver stations (BTS) around it.

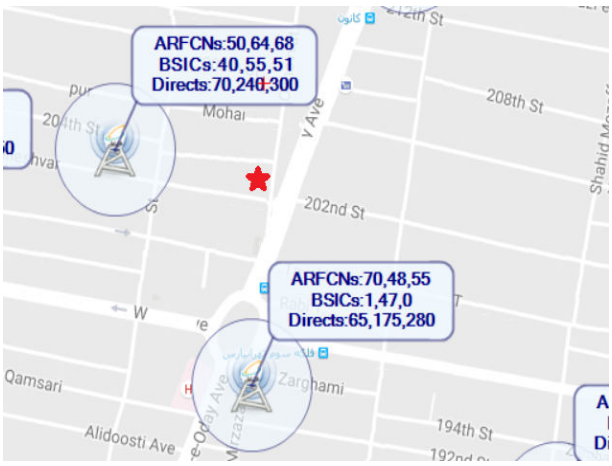

FIGURE 3. The location of the starred receiver and transmitters.

According to Fig. 3, each BTS point represents three base stations including the parameters ARFCN, base station identity code (BSIC) and Direct denoting the frequency, identity code, and the angle of the antennas, respectively. The angle is in degree mode with respect to the north of the map. The base stations with ARFCN = 50 and ARFCN = 48 are employed for testing. The receiver is approximately located in the main-lobe of the BTS with ARFCN = 50, and in the back-lobe of the BTS with ARFCN = 48.

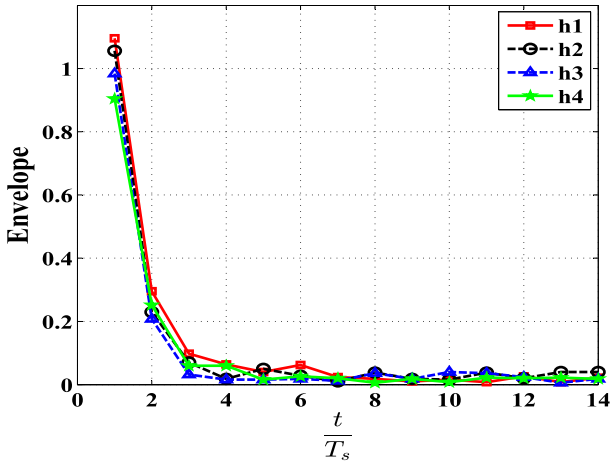

FIGURE 4. Four ensembles of the random process $|h(n)|$.

The central frequencies of the transmitter in the base stations with ARFCN = 50 and ARFCN = 48 are 945 MHz and 944.6 MHz, respectively. In both cases, the signal is recorded using a universal software radio peripheral (USRP), B210 model, and the channel is estimated 3000 times based on 14 taps. Fig. 4 shows four ensembles of the random process $|h(n)|$ with 14 taps. In the following, all taps are compared using statistical tests.

C. ADAPTATION OF PRACTICAL DATA TO FADING MODELS

Firstly, the received samples from the signal of the BTS with ARFCN = 50 are investigated. Note that, the samples are from the main-lobe of the antenna. To compare the adaptation of the various PDFs, the parameters related to the PDFs are estimated using the maximum likelihood estimation (MLE) method, and then, the P-value is calculated based on the obtained PDFs and the received samples.

TABLE 5. GOF results associated with fading models based on the K-S, A-D and KLD criteria for the BTS with ARFCN = 50.

PDF	A-D	K-S	-20log KLD
Raician	.5565	0.7683	-29.42
Weibull	1.61e-7	0.0771	-24.34
GG	0.0646	0.0573	-24.12
Nakagami-m	0.0032	0.0021	-20.42
F	0.0013	5.50e-4	-20.10
GK	0.0010	4.23e-4	-19.00
Gamma	1.61e-7	2.70e-10	-14.02
$\kappa-\mu\ sh.$	0	3.22e-11	-14.03
$\eta-\mu$	0	3.22e-11	-14.03
Rayleigh	1.61e-7	5.70e-52	-10.79
K	0	4.99e-56	-9.09
$\kappa-\mu$	0	0	Inf

If the alpha level exceeds 5% for the result of a test, the null hypothesis is confirmed, i. e., the PDF confirms with the data. In other words, when the P-value exceeds 5%, the adaptation of the related PDF to the received samples is confirmed. Table 5 shows the results of GOF for the fading models based on the K-S, A-D and KLD criteria. According to the results of the Table 5, the fifth tap of the BTS channel

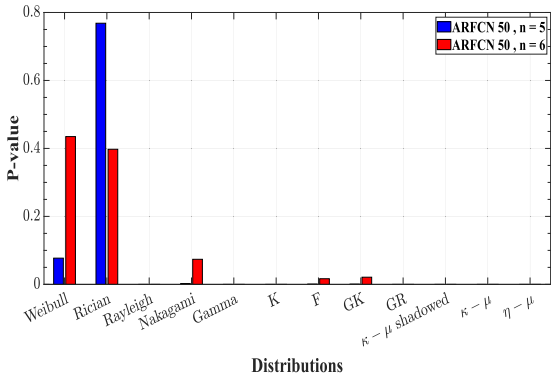

FIGURE 5. Comparing the values of K-S test in the BTS channel with ARFCN = 50.

with ARFCN = 50 confirms the Rician distribution based on the highest level of alpha. In addition, the Weibull and Nakagami-m distribution functions also sound appropriate for the data. To have a better comparison, Fig. 5 shows the P-value in the K-S test for the fifth and sixth taps.

Overally, the results show that the taps 2 and 3 do not match any of the PDFs. The taps 4, 5 and 6 confirm the Rician and Weibull distributions. Note that, the fifth tap confirms many of the distributions and the eighth tap confirms only the F, GK and K distributions. As predicted, the results confirm the adaptation of the Rician, Nakagami and Weibull fading models when the transmitter antenna lies in the direction of the receiver antenna in LOS and NLOS environment. Nevertheless, the models such as F and K also match the statistical model related to the received samples suitably.

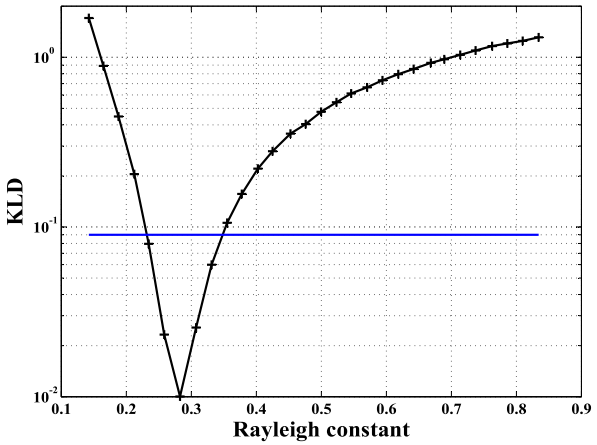

FIGURE 6. Comparing the adaptation of Rayleigh and K distributions to the received samples for the 5th tap of the BTS with ARFCN = 50.

Based on the KLD criterion, the PDF obtained from the received samples is compared with two Rayleigh and K distributions, and the deviation of the related PDF from the Rayleigh and K distributions is explored [23]. Fig. 6 compares the adaptation of the Rayleigh and K distributions to the samples related to the fifth tap of the BTS channel with ARFCN = 50. The horizontal axis is the constant of the Rayleigh distribution and the vertical axis shows the KLD. The best compatibility of the samples with the Rayleigh distribution is obtained for a Rayleigh constant of 0.28. However, the best compatibility with the K distribution is happened for the parameters c = 20 and d = 15.697. As expected, it is concluded that deviation of the samples from Rayleigh is less than the deviation from the K function.

TABLE 6. GOF results associated with fading models based on the K-S, A-D and KLD criteria for the BTS with ARFCN = 48.

PDF	A-D	K-S	-20log KLD
$\kappa - \mu\, sh.$	0.9751	0.9535	-23.64
GG 0.3	0.7908	0.9046	-21.34
F	0.0585	0.0887	-21.93
GR	0.0592	0.1527	-20.68
$\eta - \mu$	0.1014	0.0787	-22.47
GK	7.19e-04	4.11e-04	-19.21
K	7.04e-04	3.85e-04	-19.20
$\kappa - \mu$	1.90e-04	1.12e-04	-18.72
Gamma	2.23e-04	1.02e-04	-18.83
Weibull	2.45e-07	7.98e-05	-15.96
Nakagami-m	2.45e-07	1.44e-18	-10.91
Rayleigh	2.45e-07	2.98e-122	-3.54
Raician	2.45e-07	2.85e-122	-3.54

The second experiment is repeated for the BTS with ARFCN = 48 using a similar method. Given that the receiver is located at the back-lobe of the transmitter antenna, and the signal is received by the receiver in NLOS environment and after being collided with and reflected from different obstacles, and the density of the received signals is lower, the experiment should be naturally different from the previous one. Table 6 includes the statistical tests associated with the seventh tap of the channel. An alpha level over 5% confirms the adaptation of the distribution. Thus, the P-value more than 0.05 confirms the adaptation of the related PDF.

Given the desirable results obtained for the F and GR distributions compared to other models, these two distributions are compatible with the data in the second experiment. The bar chart in Fig. 7 also shows the comparison of the seventh and tenth taps of the channel.

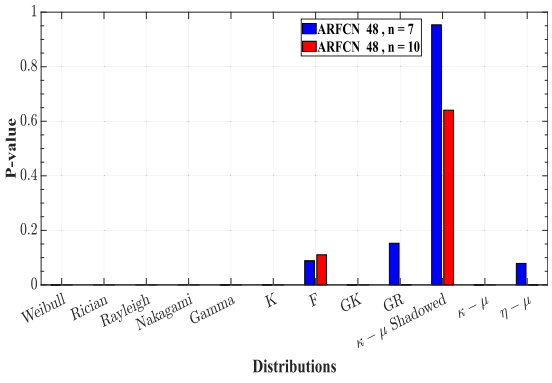

FIGURE 7. Comparing the values of K-S test in the BTS channel with ARFCN = 48.

The $\kappa - \mu$ shadowed distribution is observed to be the only distribution compatible with the data, which is yielded

significantly successful test results. The F and GR distributions are also appropriate to some extent. However, the other distributions such as K and GK that were introduced as the suitable PDFs in the conventional methods [3], [22], exhibit unreliable results.

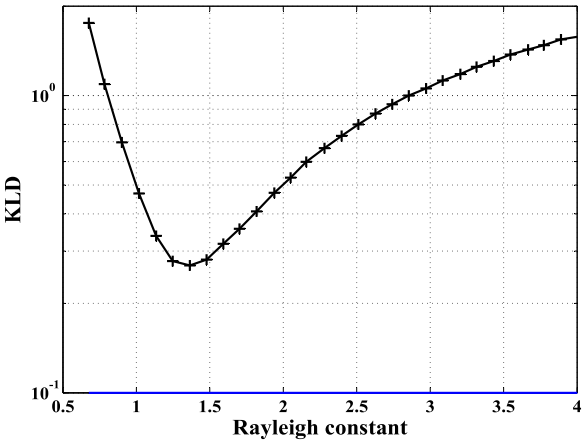

FIGURE 8. Comparing the adaptation of Rayleigh and K distributions to the received samples for the 7th tap of the BTS with ARFCN = 48.

Fig. 8 compares the adaptation of the Rayleigh and K distributions to the samples related to the seventh tap of the BTS channel with ARFCN = 48. The best compatibility of the samples with the Rayleigh distribution is obtained for a Rayleigh constant of 1.39. However, the best compatibility with the K distribution is happened for the parameters $c = 1.089$ and $d = 0.9806$, and the KLD is 0.5. Thus, the adaptation to the K distribution results in a lower KLD. According to Fig. 8, the deviation of the samples from the K function is lower than that of the Rayleigh.

D. COMPARING THE RESULTS OF THE GG DISTRIBUTION WITH THE OTHER ONES

Now, the flexibility of the GG distribution is investigated. To compare the adaptation of the previous distributions to the GG distribution, the MLE method is employed again to estimate the parameters of the GG distribution. Based on Table 5, the fifth and sixth taps of the BTS channel with ARFCN = 50 on the LOS / NLOS channel confirm the Rician distribution, as expected, with the strongest alpha level. However, it is noticeable that the GG function also passes the alpha level of 5% in this case as demonstrated in Fig. 9. Thus, the reliability of GG function is also concluded in this condition. For better comparison, Fig. 10 depicts the various PDFs estimated based on the MLE method. The parameters of each PDF are obtained to have the best fit with the received samples.

In the next test performed on BTS with ARFCN = 48 on the NLOS channel, as shown in Fig. 11, the GG function passes the alpha level of 5%, and it is concluded that this model is also in compliance with these conditions.

According to the results of Table 7, the seventh tap of the BTS with ARFCN = 48 confirms the GG distribution with

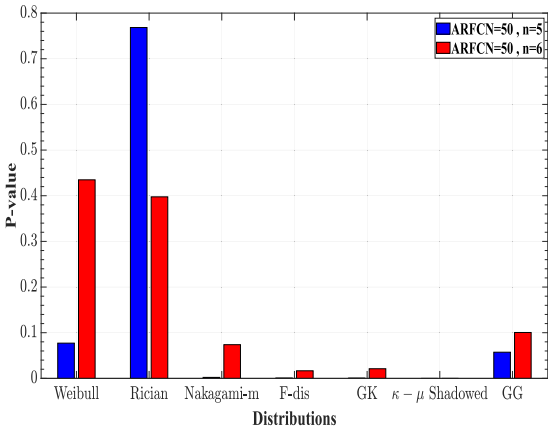

FIGURE 9. Comparing the values of K-S test in the BTS channel with ARFCN = 50 for the GG model.

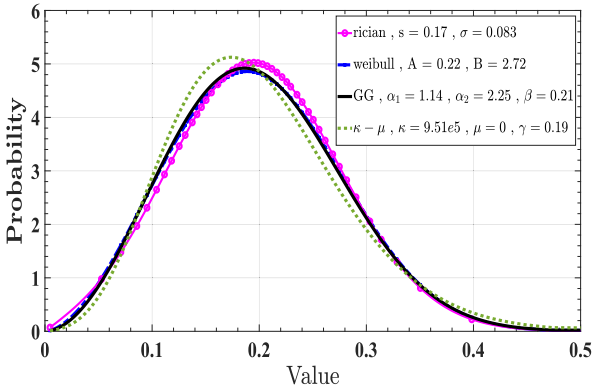

FIGURE 10. Illustrating the GG function compared with other functions in the BTS channel with ARFCN = 50.

the highest alpha level. Several tests in these conditions show that the GG function offers the highest compatibility with the fading model comparing to other closed-form functions when the transmitter antenna is not along that of the receiver and the reflected signals received by the receiver have a low density.

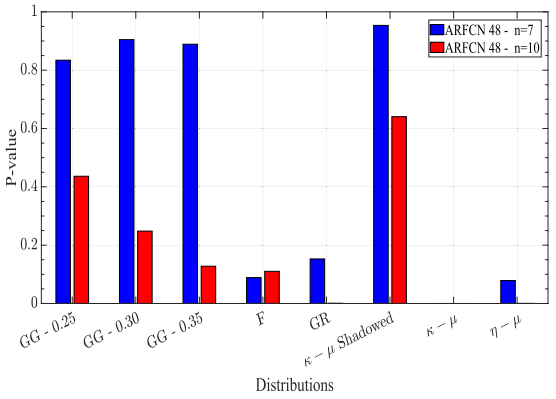

FIGURE 11. Comparing the values of K-S test in the BTS channel with ARFCN = 48 for the GG model.

On the other hand, to have a better comparison, Fig. 11 shows the result of the K-S test for the seventh and tenth taps.

TABLE 7. Comparing the degree of compatibility of the samples with the GG distribution for different values of the shape parameter (α_2).

PDF	A-D	K-S	-20log KLD
$\kappa-\mu\ sh.$	0.9751	0.9535	-23.64
GG 0.30	0.7908	0.9046	-21.34
GG 0.35	0.8724	0.8889	-22.18
GG 0.25	0.6177	0.8342	-20.47
GR	0.0592	0.1527	-20.68
F	0.0585	0.0887	-21.93
$\eta-\mu$	0.1014	0.0787	-22.47
$\kappa-\mu$	1.90e-04	1.12e-04	-18.72

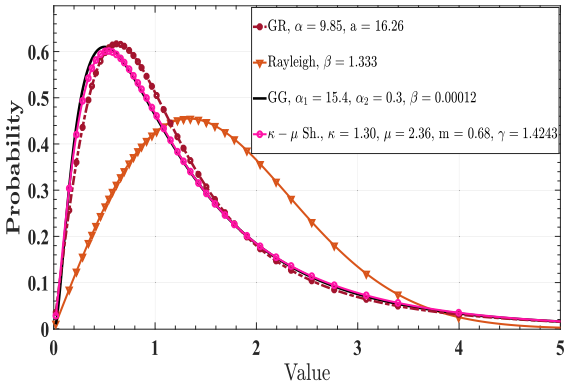

FIGURE 12. Illustrating the GG function with a shape parameter (α_2) of 0.3 compared with other functions in the BTS channel with ARFCN = 48.

Based on the Fig. 11, the previously-introduced models such as the F and GR, which were well adapted to model the different conditions of fading, present a very low level of similarity compared to the GG model. Fig. 12 depicts the various PDFs estimated based on the MLE method. The parameters of each PDF are obtained to have the best fit with the received samples. For example, the values 0.3, 15.4 and 0.00012 are estimated for α_1, α_2 and β parameters of the GG distribution, respectively. To compare the EDF value of the various models based on real data, and observe the flexibility of the GG function in both tests, refer to Appendix A.

Note that, only the complicated models such as $\kappa-\mu$ shadowed distribution, provide significant results, in which case the GG results are also similar to them (see Appendix B).

Finally, Fig. 13 shows the scatter plot for the probability of the best fitting versus the GG parameter (α_2) related to the

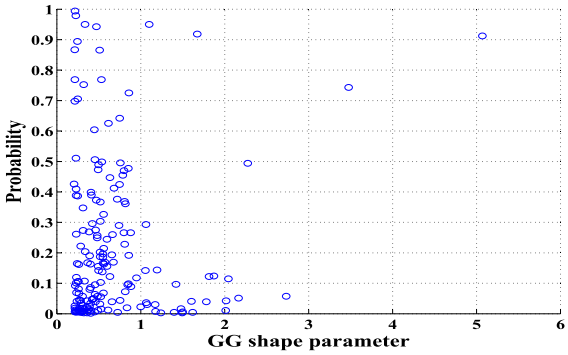

FIGURE 13. The scatter plot for the probability of the best fitting versus the GG parameter (α_2).

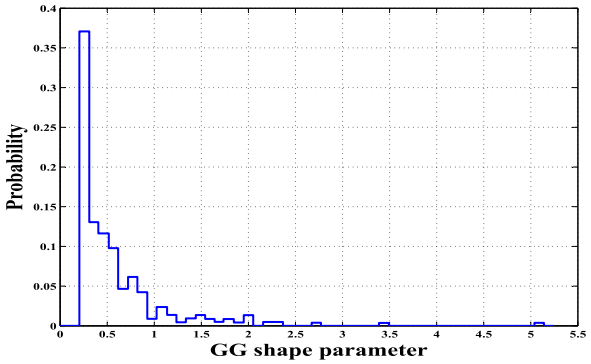

FIGURE 14. The mean of the best fitting probability versus the GG parameter (α_2).

BTS with ARFC = 48. Fig. 14 also shows the mean of the best fitting probability versus the GG parameter (α_2) related to the same BTS. As observed in Figs. 13 and 14, the highest density of the shape parameter (α_2) of the GG function lies between zero and one.

V. CONCLUSION

In this paper, the flexibility of the GG distribution is investigated for modeling the long-term fading, and the combined long and short-term fading, and some noticeable results are obtained. The results obtained from comparing the JSD and ISE tests related to the K, GR and $\kappa-\mu$ shadowed models show that the GG model presents a better similarity with the RL model. Thus, it is proposed that the GG model is employed for modeling the long-term fading instead of the RL. On the other hand, in the LOS / NLOS channel, the GG model adaptation with the real data is shown. It is also concluded that the results related to the GG model are close to the Rician model based on JSD test. Finally, the fading models in NLOS channels is also investigated, when the receiver is located at the back-lobe of the transmitter antenna, and the density of the received signals is low. The channel is estimated using the train data in the SCH bursts of the GSM signals. Two types of channel are studied. The main difference of them is related to the angle between the transmitter and the receiver antennas. In the first experiment, the receiver antenna is aligned with the main-lobe of the transmitter, whereas in the second one, the receiver receives the reflected signal from the back-lobe of the transmitter antenna. As expected, the Rician, Weibull and GG are the most compatible models with the fading model of the samples in the first experiment. The KLD results also show that the GG model is adapted with the real data and that the related results are close to the Rician and Weibull models. In the second experiment, the K and GK models are expected to present a better performance, while the F, GR and $\kappa-\mu$ shadowed model are the most compatible models compared to the other models. It is worth noting that the GG model is significantly compatible with the fading model of the samples and is better than all other closed-form models for a shape parameter (α_2) between zero and one.

The results confirm the adaptation of the GG model to the long-term and composite short-term and long-term fading.

APPENDIX

A. EDF VALUES COMPARISON

In addition to depicting the best fitted curves of the various PDFs in Figs. 10 and 12, the numerical differences of these functions, related to the test discussed in section IV-D, are also demonstrated in Figs. 15 and 16. The EDF value of the various models based on real data for transmitter with ARFCN = 50 is shown in Fig. 15, and the same value for transmitter with ARFCN = 48 is depicted in Fig. 16. It is obvious that the functions whose EDF is close to the zero axis have the best fit with the real data.

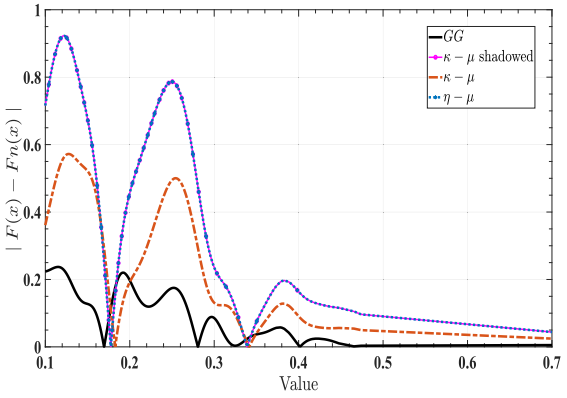

FIGURE 15. The EDF values comparison among the various models based on real data for transmitter with ARFCN = 50.

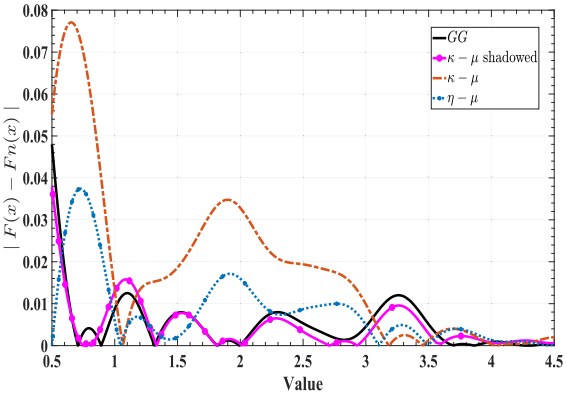

FIGURE 16. The EDF values comparison among the various models based on real data for transmitter with ARFCN = 48.

B. $\alpha - \kappa - \mu$ SHADOWED DISTRIBUTION

There are models such as $\alpha-\eta-\mu$, $\alpha-\kappa-\mu$ and $\alpha-\kappa-\mu$ shadowed distributions that have a good fit in different fading modes [34]. However, some models do not have a closed-form, and the number of the related parameters is sometimes great, therefore, they have more computational complexity. As an example, the $\alpha - \kappa - \mu$ shadowed model, which includes a large range of fading models, is compared to the GG function in the following.

Let γ be a random variable that statistically is $\alpha - \kappa - \mu$ shadowed distributed with mean $\bar{\gamma}=E[\gamma]$ and non-negative real shape parameters α, κ, μ and m, i. e., $\gamma \sim S_{\alpha\kappa\mu m}(\bar{\gamma};\alpha,\kappa,\mu,m)$, and the related PDF is given by [34]:

$$f_\gamma(\gamma) = \frac{m^m\alpha}{2c^\mu\Gamma(\mu)(\mu\kappa+m)^m\bar{\gamma}}\left(\frac{\gamma}{\bar{\gamma}}\right)^{\frac{\alpha\mu}{2}-1} \times \exp\left(-\frac{1}{c}\left(\frac{\gamma}{\bar{\gamma}}\right)^{\frac{\alpha}{2}}\right) \times {}_1F_1\left(m,\mu;\frac{\mu\kappa}{c(\mu\kappa+m)}\left(\frac{\gamma}{\bar{\gamma}}\right)^{\frac{\alpha}{2}}\right), \quad (23)$$

where ${}_1F_1(.)$ is the confluent hypergeometric function [16], and:

$$c = \left(\frac{\Gamma(\mu)(\mu\kappa+m)^m}{m^m\Gamma\left(\mu+\frac{2}{\alpha}\right){}_2F_1\left(m,\mu+\frac{2}{\alpha};\mu;\frac{\mu\kappa}{\mu\kappa+m}\right)}\right)^{\alpha/2}. \quad (24)$$

Table 8 presents the comparison among the $\alpha - \kappa - \mu$ shadowed model and other ones for transmitter with ARFCN = 50 in LOS / NLOS mode. Table 9 also shows the results for transmitter with ARFCN = 48 in NLOS mode.

TABLE 8. GOF results associated with fading models based on the K-S, A-D and KLD criteria for the BTS with ARFCN = 50.

PDF	A-D	K-S	-20log KLD
Raician	.5565	0.7683	-29.42
$\alpha-\kappa-\mu\, sh.$	0.2811	0.2372	-27.75
Weibull	1.61e-7	0.0771	-24.34
GG	0.0646	0.0573	-24.12
Nakagami-m	0.0032	0.0021	-20.42
$\kappa-\mu\, sh.$	0	3.22e-11	-14.03

TABLE 9. GOF results associated with fading models based on the K-S, A-D and KLD criteria for the BTS with ARFCN = 48.

PDF	A-D	K-S	-20log KLD
$\alpha-\kappa-\mu\, sh.$	0.9851	0.9844	-23.40
$\kappa-\mu\, sh.$	0.9751	0.9535	-23.64
GG 0.3	0.7908	0.9046	-21.34
F	0.0585	0.0887	-21.93
GR	0.0592	0.1527	-20.68
$\eta-\mu$	0.1014	0.0787	-22.47

TABLE 10. The complexity comparing of the flexible models in various fading modes.

PDF	Parameters	Form	Flexibility	
			ARFCN=50	ARFCN=48
$\alpha-\kappa-\mu\, sh.$	$\bar{\gamma},\alpha,\kappa,\mu,m$	non-closed	passed	passed
$\kappa-\mu\, sh.$	$\bar{\gamma},\kappa,\mu,m$	non-closed	failed	passed
GG	α_1,α_2,β	closed	passed	passed

Based on the Tables 8 and 9, the flexible models that are reliable for both NLOS mode and combined LOS / NLOS one are only the GG and $\alpha - \kappa - \mu$ shadowed functions. However, based on the Table 10, the GG function has a simpler, closed-form and less complex function than the other ones.

REFERENCES

[1] M. K. Simon and M. S. Alouini, *Digital Communication Over Fading Channels*, vol. 95. Hoboken, NJ, USA: Wiley, 2005.

[2] W. Wang, J. Y. Xiong, and Z. L. Zhu, "A new NLOS error mitigation algorithm in location estimation," *IEEE Trans. Veh. Technol.*, vol. 54, no. 6, pp. 2048–2053, Nov. 2005.

[3] P. Bithas, P. Mathiopoulos, and S. Kotsopoulos, "Diversity reception over generalized-K (KG) fading channels," *IEEE Trans. Wireless Commun.*, vol. 6, no. 12, pp. 4238–4243, Dec. 2007.

[4] S. Suljović, D. Krstić, S. Maričić, S. Zdravković, V. Milenković, and M. Stefanović, "Level crossing rate of SC receiver over gamma shadowed weibull multipath fading channel," *Tech. Gazette*, vol. 23, no. 6, pp. 1579–1584, Dec. 2016.

[5] P. Mohana Shankar, "A general statistical model for ultrasonic backscattering from tissues," *IEEE Trans. Ultrason., Ferroelectr., Freq. Control*, vol. 47, no. 3, pp. 727–736, May 2000.

[6] T. Eltoft, "The Rician inverse Gaussian distribution: A new model for non-Rayleigh signal amplitude statistics," *IEEE Trans. Image Process.*, vol. 14, no. 11, pp. 1722–1735, Nov. 2005.

[7] E. Gómez-Déniz and L. Gómez-Déniz, "A generalisation of the Rayleigh distribution with applications in wireless fading channels," *Wireless Commun. Mobile Comput.*, vol. 13, no. 1, pp. 85–94, Jan. 2013.

[8] L. Moreno-Pozas, F. J. Lopez-Martinez, J. F. Paris, and E. Martos-Naya, "The κ-μ shadowed fading model: Unifying the κ-μ and η-μ distributions," *IEEE Trans. Veh. Technol.*, vol. 65, no. 12, pp. 9630–9641, Dec. 2016.

[9] J. F. Paris, "Statistical characterization of κ–μ shadowed fading," *IEEE Trans. Veh. Technol.*, vol. 63, no. 2, pp. 518–526, Feb. 2014.

[10] J. Malhotra, A. K. Sharma, and R. S. Kaler, "On the performance analysis of wireless receiver using generalized-gamma fading model," *Ann. Telecommun.*, vol. 64, nos. 1–2, pp. 147–153, Feb. 2009.

[11] E. Yaacoub and Z. Dawy, "A survey on uplink resource allocation in OFDMA wireless networks," *IEEE Commun. Surveys Tuts.*, vol. 14, no. 2, pp. 322–337, 2nd Quart., 2012.

[12] F. J. Massey, "The Kolmogorov–Smirnov test for goodness of fit," *J. Amer. Stat. Assoc.*, vol. 46, no. 253, pp. 68–78, Mar. 1951.

[13] S. Kullback and R. A. Leibler, "On information and sufficiency," *Ann. Math. Statist.,*, vol. 22, no. 1, pp. 79–86, 1951.

[14] T. W. Anderson and D. A. Darling, "A test of goodness of fit," *J. Amer. Stat. Assoc.*, vol. 49, no. 268, pp. 765–769, 1954.

[15] M. D. Yacoub, "The κ-μ and theη-μ distribution," *IEEE Antennas Propag. Mag.*, vol. 49, no. 1, pp. 68–81, Feb. 2007.

[16] M. Abramowitz and I. A. Stegun, *Handbook of Mathematical Functions*. New York, NY, USA: Dover, 1995.

[17] F. J. Lopez-Martinez, J. F. Paris, and J. M. Romero-Jerez, "The κ-μ shadowed fading model with integer fading parameters," *IEEE Trans. Veh. Technol.*, vol. 66, no. 9, pp. 7653–7662, Sep. 2017.

[18] X. Li, J. Li, L. Li, J. Jin, J. Zhang, and D. Zhang, "Effective rate of MISO systems over κ–μ shadowed fading channels," *IEEE Access*, vol. 5, pp. 10605–10611, 2017.

[19] J. Zhang, Z. Wang, L. Dai, and W. H. Gerstacker, "Effective capacity of communication systems over κ—μ shadowed fading channels," *Electron. Lett.*, vol. 51, no. 19, pp. 1540–1542, Sep. 2015.

[20] P. Beckmann, "Rayleigh distribution and its generalizations," *Radio Sci. J. Res.*, vol. 68D, no. 9, p. 927, Sep. 1964.

[21] E. Jakeman, "Speckle with a small number of scatterers," *Opt. Eng.*, vol. 23, pp. 453–461, Jul/Aug. 1984.

[22] E. Jakeman and P. Pusey, "A model for non-Rayleigh sea echo," *IEEE Trans. Antennas Propag.*, vol. AP-24, no. 6, pp. 806–814, Nov. 1976.

[23] G. V. Weinberg and V. G. Glenny, "Optimal Rayleigh approximation of the k-distribution via the kullback-leibler divergence," *IEEE Signal Process. Lett.*, vol. 23, no. 8, pp. 1067–1070, Aug. 2016.

[24] S. K. Yoo, S. L. Cotton, P. C. Sofotasios, M. Matthaiou, M. Valkama, and G. K. Karagiannidis, "The Fisher-Snedecor $\mathcal{F}$ distribution: A simple and accurate composite fading model," *IEEE Commun. Lett.*, vol. 21, no. 7, pp. 1661–1664, Jul. 2017.

[25] S. Suksaengrakcharoen and W. Bodhisuwan, "A new family of generalized gamma distribution and its application," *J. Math. Statist.*, vol. 10, no. 2, pp. 211–220, Feb. 2014.

[26] A. A. Ahmed, "On new method of estimation of parameters of size-biased generalized Gamma distribution and its structural properties," *IOSR-J. Math.*, vol. 5, no. 2, pp. 34–40, Mar. 2013.

[27] A. Abdi and M. Kaveh, "K distribution: An appropriate substitute for Rayleigh-lognormal distribution in fading-shadowing wireless channels," *Electron. Lett.*, vol. 34, no. 9, p. 851, Apr. 1998.

[28] J. Lin, "Divergence measures based on the Shannon entropy," *IEEE Trans. Inf. Theory*, vol. 37, no. 1, pp. 145–151, Jan. 1991.

[29] A. W. Bowman, "An alternative method of cross-validation for the smoothing of density estimates," *Biometrika*, vol. 71, no. 2, pp. 353–360, Aug. 1984.

[30] A. Abdi and M. Kaveh, "Comparison of DPSK and MSK bit error rates for K and Rayleigh-lognormal fading distributions," *IEEE Commun. Lett.*, vol. 4, no. 4, pp. 122–124, Apr. 2000.

[31] R. B. D'Agostino, *Goodness-of-Fit-Techniques*, vol. 68. Boca Raton, FL, USA: CRC Press, 1986.

[32] L. Tong, G. Xu, and T. Kailath, "Blind identification and equalization based on second-order statistics: A time domain approach," *IEEE Trans. Inf. Theory*, vol. 40, no. 2, pp. 340–349, Mar. 1994.

[33] *Digital Cellular Telecommunications System (Phase 2+); Multiplexing and Multiple Access on the Radio Path (GSM 05.02 Version 8.5.1 Release 1999*, document ETSI EN 300 908, V8.5.1, Nov. 2000.

[34] P. Ramirez-Espinosa, J. M. Moualeu, D. Benevides da Costa, and F. J. Lopez-Martinez, "The $\alpha - \kappa - \mu$ shadowed fading distribution: Statistical characterization and applications," Apr. 2019, *arXiv:1904.05587*. [Online]. Available: https://arxiv.org/abs/1904.05587

ZABIHOLLAH HASANSHAHI was born in Shiraz, Iran, in July 1974. He received the B.Sc. and M.Sc. degrees in electrical engineering from the Malek Ashtar University of Technology (MUT), Tehran, Iran, in 2000 and 2011, respectively. He is currently pursuing the Ph.D. degree. Since April 2001, he has been with the Telecommunication Research Institute, Tehran, where he designed and implemented communication systems, such as net monitoring for quality of service analyzing in cellular networks. His research interests are statistical signal processing, cellular and satellite communication, wave propagation, and fading phenomena. He is currently involved with system identification and wireless communications and digital signal processing.

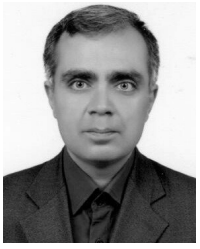

PAEIZ AZMI (Senior Member, IEEE) was born in Tehran, Iran, in April 1974. He received the B.Sc., M.Sc., and Ph.D. degrees in electrical engineering from the Sharif University of Technology (SUT), Tehran, in 1996, 1998, and 2002, respectively. From 1999 to 2001, he was with the Advanced Communication Science Research Laboratory, Iran Telecommunication Research Center (ITRC), Tehran. From 2002 to 2005, he was with the Signal Processing Research Group, ITRC. Since September 2002, he has been with the Electrical and Computer Engineering Department, Tarbiat Modares University, Tehran, and became an Associate Professor, in January 2006, where he is currently a Full Professor. His current research interests include modulation and coding techniques, digital signal processing, wireless communications, resource allocation, molecular communications, and estimation and detection theories.

MOHAMMAD HOSSEIN GHOLIZADEH was born in Rafsanjan, Iran, in 1985. He received the B.Sc. degree from the Isfahan University of Technology, Isfahan, Iran, in 2007, and the M.Sc. and Ph.D. degrees from the Amirkabir University of Technology, Tehran Polytechnic, Tehran, Iran, in 2010 and 2015, respectively, all in electrical engineering. He is currently an Assistant professor with the Electrical Engineering Department, Vali-e-Asr University of Rafsanjan, Rafsanjan. His research interests are radar and sonar signal processing. He is currently involved with statistical image and voice processing, system identification, and wireless communications.

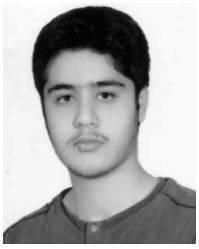

MOHAMMAD KHAJEZADEH was born in Shiraz, Iran, in 1992. He received the B.Sc. degree in electrical engineering from Shiraz University, Shiraz, in 2014, and the M.Sc. degree in telecommunication engineering from the Amirkabir University of Technology, Tehran, in 2016. He is currently working on MAC and physical layer in different Standards like LTE, 5G, and WiMax at the Radar Laboratory, Amirkabir University of Technology. His research interests include wave propagation and fading phenomena, beamforming in satellite communication, and statistical signal processing as applied to sensor array systems.